Ecological Modelling 404 (2019) 69–82

Contents lists available at ScienceDirect

Ecological Modelling

journal homepage: www.elsevier.com/locate/ecolmodel

Sensory perception plays a larger role in foraging efficiency than heavy-tailed movement strategies

Diana E. LaScala-Gruenewald[a,*], Rohan S. Mehta[b], Yu Liu[c], Mark W. Denny[a]

[a] Hopkins Marine Station, Stanford University, Pacific Grove, California, United States
[b] Department of Biology, Stanford University, Stanford, California, United States
[c] Department of Mathematics, Uppsala University, Uppsala, Sweden

ARTICLE INFO

Keywords:
agent-based model
destructive foraging
environmental heterogeneity
Lévy walk
optimal search
sensory perception

ABSTRACT

Animals must balance their rates of energetic intake and expenditure while foraging. Several mathematical models have been put forward as energetically optimal foraging strategies when the food environment is sparse (i.e., the distance between food patches in the environment is much larger than the distance from which the forager can perceive food). In particular, Lévy walks with a power law exponent approaching 1 are considered optimal for destructive foragers. However, these models have yet to explore the role of sensory perception in foraging success as the distance between food patches approaches the distance from which the forager can perceive food. Here, we used an agent-based modeling approach to address this question. Our results concur that lower values of the power law exponent (i.e. values approaching 1) result in the most food found, but in contrast to previous studies, we note that, in many cases, lower exponents are not optimal when we consider food found per unit distance traveled. For example, higher values of the exponent resulted in comparable or higher foraging success relative to lower values when the forager's range of sensory perception was restricted to an angle ± 30° from its current heading. In addition, we find that sensory perception has a larger effect on foraging success than the power law exponent. These results suggest that a deeper examination of how animals perceive food sources from a distance may affect longstanding assumptions regarding the optimality of Lévy walk foraging patterns, and lend support to the developing theoretical shift towards models that place increasing emphasis on how organisms interact with their environments.

1. Introduction

All animals must find food in an energetically-feasible manner in order to survive. Optimal Foraging Theory (OFT) holds that animals seek to maximize their net rate of energy intake – the difference between their energetic benefit (in terms of calories, nutrients, etc.) and their energetic expenditure over time – while searching for, handling, consuming, and digesting food (MacArthur & Pianka, 1966). OFT transformed the field of foraging ecology, stimulating both empirical and theoretical work on diet, patch selection, and residence time (Pyke, 1984). However, the issue of how animals should optimally move between food patches was initially underrepresented in the literature (Pyke, 1978, 1984, 2015; but see Cody, 1971; Root & Kareiva, 1984; Siniff & Jesson, 1969; Smith, 1973). Researchers observed that animals across taxa performed Area Restricted Search (ARS): they responded to encounters with food patches by transitioning from a rapid, directed movement regime to one that was slow and tortuous (e.g. Banks, 1957; Benhamou & Bovet, 1989; Bond, 1980; Fielden et al., 1990; Hassell & May, 1973; Mueller et al., 2011; Pyke, 1978; Thomas, 1974; Weimerskirch et al., 2002; White et al., 1984). But a true synthesis of optimal movement between food patches remained incomplete.

Initial efforts to provide a theoretical basis for the observed ARS patterns drew from simple random walk (SRW) models (Cody, 1971; Kareiva and Shigesada, 1983; Pyke, 1978; Siniff and Jesson, 1969; Smith, 1973; Turchin, 1998; Viswanathan et al., 2011), in which an animal's trajectory is discretized into a series of linear steps. The step lengths are drawn from an exponential distribution, and the step directions are chosen at random, resulting in a forager whose mean squared displacement grows linearly with time and whose changes in direction are uncorrelated (Dray et al., 2010; Pyke, 2015; Viswanathan et al., 2011). Correlated random walk (CRW) models elaborated on SRWs (Benhamou, 2007; Codling et al., 2008) by incorporating some degree of correlation between the directions of successive steps. This adjustment helped simulate the directional persistence that is

* Corresponding author. Present Address at: Leigh Marine Laboratory, University of Auckland, Leigh, New Zealand
E-mail address: d.lascala-gruenewald@auckland.ac.nz (D.E. LaScala-Gruenewald).

https://doi.org/10.1016/j.ecolmodel.2019.02.015
Received 19 October 2018; Received in revised form 24 February 2019; Accepted 26 February 2019
Available online 10 April 2019

characteristic of the movements of most organisms (Pyke, 2015). Most recently, Lévy walks (also called Lévy flights) have been proposed as an alternative optimal search strategy (Viswanathan et al., 1999, 2000). One way in which Lévy walks differ from SRWs and CRWs is that the length of each step is chosen from a probability distribution given by the power law distribution

$$P(x) = Cx^{-\alpha}, \quad (1)$$

where C is a normalizing constant, x is the step length and $\alpha > 1$ (Viswanathan et al., 2000, 1999). As α increases beyond 3, the Lévy walk converges on Brownian motion; when $\alpha < 3$, a Lévy walker has higher probabilities of taking very long steps than does a simple or correlated random walker.

In 1999, Viswanathan et al. proposed the Lévy Flight Foraging Hypothesis (LFFH), which suggests that Lévy walks with particular values of α should maximize the quantity of food found per distance traveled over time for foragers in environments with sparse, randomly distributed food patches (Viswanathan et al., 1999, 2000). In the case of nondestructive foraging, where food patches returned instantaneously to their ungrazed state after an encounter with a forager, $\alpha = 2$ was optimal. In the case of destructive foraging, where food patches were completely depleted after an encounter with a forager, an α value approaching 1 was optimal.

Numerous subsequent studies found that a power law with an exponent of 2 best modeled *in situ* foraging behavior in a wide variety of taxa, apparently in support of the LFFH (e.g. Bartumeus et al., 2010; de Jager et al., 2011; Franks et al., 2010; Raichlen et al., 2013; Reynolds et al., 2014; Seuront & Stanley, 2014; Sims et al., 2008). However, other researchers reported contrasting results (Reynolds, 2015) and raised concerns regarding the statistical procedures required to accurately identify power law distributions in empirical data (Clauset et al., 2009; Edwards, 2008; Edwards et al., 2007). When more accurate procedures were used, the outcomes of many studies in support of the LFFH were overturned (Clauset et al., 2009; Edwards, 2008; Edwards et al., 2007). For example, the foraging times of unfenced deer (*Dama dama*) were initially found to conform to a power law with $\alpha = 2$ (Edwards et al., 2007). However, reanalysis of the dataset using maximum likelihood and Akaike weights found that deer foraging times were better modeled by an exponential (rather than a power law) distribution. The same research team determined that bumblebee (*Bombus terricola*) flight distances could be reasonably fit to a power law distribution; however, they recalculated α to be 3.68 (rather than the original value of 3.5) in high food areas and 2.2 (rather than the original value of 2.0) in low food areas (Edwards et al., 2007).

While it is critical that ecologists employ accurate statistical techniques to analyze their data, it remains unclear to what extent changes in calculated α values actually reflect significant changes in the energy budgets of foraging animals. For example, in a biological system, animals whose movements are best modeled by values of α that differ only slightly may experience negligible changes in foraging success with respect to long-term fitness. In addition, α values do little to reveal the underlying mechanisms animals use when searching for food. It is reasonable, then, to question how substantial changes to calculated α values must be to reflect changes in underlying mechanisms that result in the evolution of optimal foraging behavior. In evaluating these mechanisms, one must consider the assumptions of the LFFH, and the fact that they commonly have not been met by the species and systems used to test the hypothesis in empirical studies (Pyke, 2015; Reynolds, 2015). Viswanathan et al. (1999, 2000) assumed that the directions of successive animal movements were uncorrelated; however, even very simple organisms tend to exhibit directional persistence (Pyke, 2015). Additionally, researchers have debated whether destructive or nondestructive foraging is the more realistic assumption (Pyke, 2015), and some have explored the effects of nondestructive foraging when food resources fully renew after some time lag (Raposo et al., 2003; Santos et al., 2004). Third, the LFFH specifically applies to organisms whose radius of sensory perception (r_v in Viswanathan et al., 1999, 2000) is much less than the average distance traveled between food patches in their environment (λ in Viswanathan et al., 1999, 2000). While a movement strategy modeled by a power law with $\alpha = 2$ might be optimal when $\lambda \gg r_v$, it is unclear how that optimal strategy shifts as λ approaches r_v. Although numerous authors have stated that the influence of α on foraging efficiency should decrease as r_v/λ approaches 1 (e.g. Bartumeus et al., 2008a; James et al., 2011; Viswanathan et al., 1999, 2000), this has not been explicitly investigated. Finally, an optimal movement strategy may be influenced by other factors not considered by Viswanathan et al. (1999, 2000) and other, similar studies. For example, many animals do not perceive food patches equally well in all directions; rather, they tend to perceive food patches that are in front of them, where the majority of their sensory organs are located (Olden et al., 2004; Pelseneer, 1906; Zollner & Lima, 1999).

In many studies of foraging behavior (see, for example: Cody, 1971; Siniff & Jesson, 1969; Turchin, 1998; Viswanathan et al., 1999), agent-based models (ABMs) have provided valuable supplements to purely analytical and empirical investigations. ABMs are flexible modeling frameworks that examine the properties that emerge from the actions of individual agents (Railsback and Grimm, 2011; Tang and Bennett, 2010). In the context of foraging behavior, agents search for food on a simulated landscape using a set of rules that may depend on the agent's internal psychological or physiological state, nearby landscape features, interactions with other agents, and a set of navigational strategies (Nathan et al., 2008; Tang and Bennett, 2010). In this study, we used an agent-based modeling framework to simulate destructive foraging during single foraging bouts. We sought to address three questions:

1) Which factor – sensory perception or foraging movement pattern as summarized by the power law exponent α – has the most influence on destructive foraging success across a range of food distributions?
2) How does the influence of α on destructive foraging success change as the forager's range of sensory perception approaches and exceeds the distance between food patches?
3) Taking both foraging movement pattern and sensory perception into account, can our model produce testable hypotheses regarding expected foraging behaviors in a model organism?

Due in part to its prominence in the literature, we expected that animal movement patterns would have the most influence on destructive foraging success, with smaller α values resulting in greater success than larger ones. However, we also expected that food availability and sensory perception would interact with animal movements, with larger values of both factors resulting in more foraging success than smaller values. We anticipated that α would have the largest effect on foraging success when the forager's range of sensory perception was much less than the distance between food patches in its landscape, and that this effect would become negligible as the forager's range of sensory perception approached and exceeded this distance. Finally, we expected that our model would allow us to generate testable hypotheses about foraging behavior in a model organism, the intertidal limpet *Patella vulgata* (Linnaeus).

2. Materials and methods

2.1. Model Description

To simulate single foraging bouts, we used an agent-based modeling framework, varying the α value of the power law distribution used to model animal foraging movements (hereafter referred to as 'foraging strategy'), the sensory abilities of the forager, and the food distribution of the landscape.

2.1.1. Landscape Generation

We generated landscapes with food distributions that ranged from relatively sparse (1% food cover) to relatively plentiful (15% food cover). These values are within the range determined to be realistic and

Table 1
Model parameters. We summarize the landscape parameters and parameters associated with the forager's movement. The parameters p, k_1 and k_2 were held constant for all simulations.

Name	Description	Units	Values
Landscape Parameters			
PC	Percent food cover of landscape	–	1, 3, 5, 7, 9, 11, 13, 15
μ	Food patch side length	grid units	1, 2, 5, 10
Forager parameters			
α	Power law parameter	–	1.1, 1.3, 1.5, 2, 2.5, 3
R	Radius of perception	grid units	0, 1, 2, 5, 10, 20
θ	Field of view	degrees	60, 360
Constant parameters			
p	Probability the forager continues forward	–	0.8
k_1	Concentration parameter for von Mises distribution centered on current heading	–	0.9
k_2	Concentration parameter for von Mises distribution centered on current heading minus 180°	–	2.3

relevant by previous studies (e.g. With & King, 1999). To do this, we created 32, 2-dimensional, bounded landscapes, and initialized each with an empty 500 × 500 grid of squares. We then randomly added non-overlapping food patches, with side lengths μ of 1, 2, 5 or 10 grid units, until the desired percent food cover was achieved. The average minimum nearest neighbor distance between food patches on the resulting landscapes ranged from 0.60 to 50.82 grid units (see Table S.1 for details).

2.1.2. Forager Characteristics

Each agent, or forager, was initialized with three inherent properties that governed its movements:, R, and θ (Table 1). Each forager drew its step lengths from a power law distribution (eq. (1)). In this distribution, the exponent α controls the size of the tail. As α increases, the size of the tail decreases, as does the probability of the forager taking very long steps (Fig. S.1).

Two parameters, R and θ, governed the ability of the forager to perceive food patches in its environment. R is the forager's radius of sensory perception. The direction of perception (θ, analogous to 'perceptual horizon' in Olden et al. 2004) was limited to the forager's current heading plus or minus $\theta/2$; $\theta = 60^{\circ}$ produced an anterior bias in perception, while $\theta = 360^{\circ}$ produced no bias. These values represented minimum and maximum cases. The parameter values used in our simulations are summarized in Table 1.

2.1.3. Simulating movement and food consumption

Our simulations were implemented in Python 2.7.9. At the beginning of each simulation, a single forager was randomly placed on a food-free square in a landscape. Initial exploratory simulations determined that $T = 1000$ time steps were sufficient to produce consistent results. For each time step (Fig. 1):

1) The forager's maximum traveling distance x was drawn from a power law distribution with parameter α.
2) The forager searched for food within the constraints of its range, R, and angle, θ, of sensory perception. During the first time step, the forager's angle of sensory perception was defined relative to an initial heading that was drawn randomly from a uniform distribution.
3) If the forager could perceive a food square, then it selected that square as its desired destination and moved toward it. If the distance to this square was less than x, the forager moved directly to the square and consumed the food. Otherwise, the forager moved a distance x along the line connecting its current position and the desired position. If the forager could perceive more than one food square, it moved toward the nearest one. In all of the above situations, the forager's heading was redefined as the angle connecting the forager and the food square.
4) If the forager could not perceive a food square, it randomly chose a heading from one of two opposite-facing von Mises distributions (Fig. 1). This strategy reflected the fact that animals tend to continue moving forward along their current path (Pyke, 2015), but also occasionally reverse direction. The von Mises distribution closely approximates a normal distribution on a circle; the probability of the forager drawing a heading of angle ϕ was defined as

$$P(\varphi|\ h, \kappa) = C(\kappa) \bullet e^{\kappa \cos(\varphi - h)}$$

where h is the angle the distribution is centered on, κ is the concentration parameter describing how much of the distribution is aggregated around h, and $C(\kappa)$ is a normalizing constant. With probability p, the forager's heading was drawn from a von Mises distribution centered on its current heading with concentration parameter k_1, and with probability 1 - p, the forager's heading was drawn from a von Mises distribution centered on the heading directly opposite from its current one, with concentration parameter k_2 (Table 1). The forager then moved incrementally along the chosen heading until a distance x was reached. If the forager perceived a food square along its path of travel, it stopped at the intermediate location. Food squares did not regenerate after consumption (i.e. foraging was destructive).

We ran the above simulation 10 times on each of the 32 landscapes for every possible combination of the parameters α, R, and θ listed in Table 1.

2.1.4. Simulation output

After each simulation, the track of the forager was recorded and two response variables were measured: the total amount of food found (F) and the benefit-cost ratio (BCR). F is the number of times a forager landed on and consumed a food patch. BCR is a measure of foraging efficiency (Houston and McNamara, 2014) that in our case increases monotonically with the forager's net rate of energetic intake (Appendix B), and is defined as the food gained by the forager per unit distance traveled over time, or:

$$BCR = \frac{\frac{F}{T}}{\frac{D}{T}} = \frac{F}{D}, \tag{2}$$

where D is the total distance traveled along the forager's path during the simulation, and $T = 1000$ time steps. We used benefit-cost ratio rather than cost-benefit ratio because some simulations resulted in $F = 0$.

2.2. Effect size of model factors

To determine how the parameters in our simulations (landscape, α, R, and θ) affected our two response metrics (F and BCR), we performed a five-factor analysis of variance (ANOVA) and a multiple linear regression with all interactions considered. We designed our landscapes with two free variables: percent cover (PC) and patch side length (μ) (Table 1). We performed ANOVAs for each response metric over these two landscape parameters as well as the movement parameters α, R, and θ. PC, μ, α, and R were represented as continuous, fixed factors,

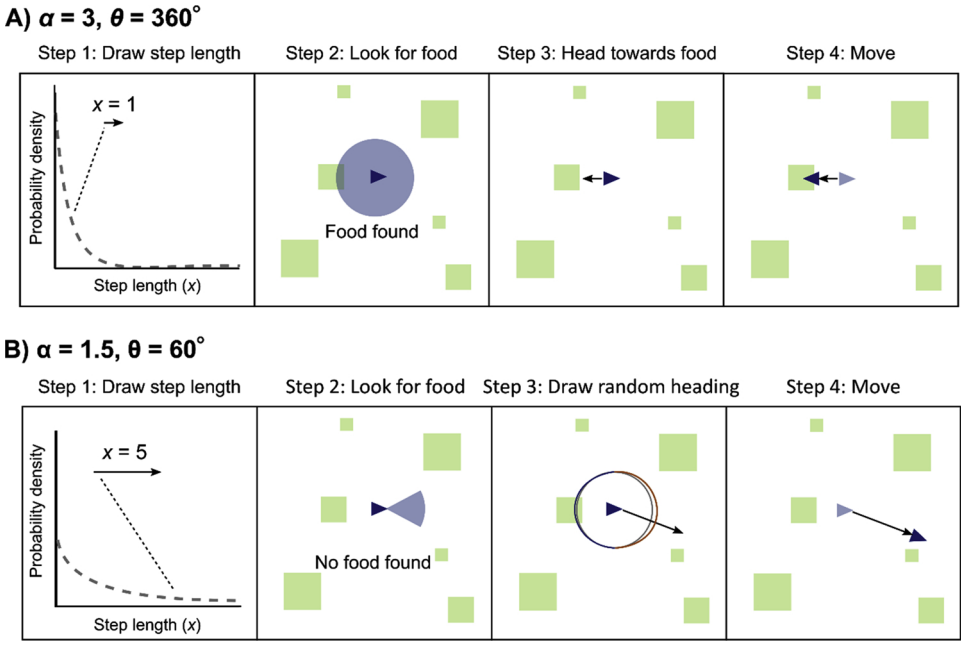

Fig. 1. Schematic of simulation steps. In scenario (A), a forager (blue triangle) draws a step length (black arrow, $x = 1$) from a power law distribution with $\alpha = 3$, looks for food within its radius and angle of sensory perception (light blue circle), finds a food square, selects a heading directed toward it (angle of black arrow), and moves. In scenario (B), a forager draws a step length ($x = 5$) from a power law distribution with $\alpha = 1.5$ and looks for food within its radius and angle of sensory perception (light blue sector), but cannot find any. It draws a heading from either a forward (orange curve with $\mu = 0^\circ$ and $k_1 = 0.9$) or backward (blue curve with $\mu = 180^\circ$ and $k_2 = 2.3$) von Mises distribution and moves.

while θ was represented as a categorical, fixed factor. All factors were centered by subtracting their mean value.

In modeling studies like ours, it is possible to perform enough simulations to achieve any level of statistical significance (White et al., 2014). Therefore, instead of reporting ANOVA *F*-statistics and regression *p*-values, we reported the proportion of variation in each response metric explained by each factor and provided the estimated regression coefficients for each factor as a measure of effect size.

To explore how the influence of α on foraging success changed as the ratio of range of sensory perception to distance between food patches shifted from 0 to greater than 1, we first calculated the average minimum nearest neighbor distance (*NND*) between patches for each of our 32 landscapes (Table S.1). We chose to use the average minimum nearest neighbor distance rather than the mean free path because we believed the former value would be more relevant to a forager moving from patch to patch. We then calculated *R/NND* for each of our simulations, a value analogous to r_v/λ in (Viswanathan et al., 1999, 2000). Next, for ease of visualization, we divided this continuous variable into five categories. The first four of these were determined by the quartiles of the ratio *R/NND*: $0 < R/NND \leq 0.18$, $0.18 < R/NND \leq 0.73$, $0.73 < R/NND \leq 2.42$, and $R/NND > 2.42$. The fifth category contained all simulations in which $R = 0$, and thus $R/NND = 0$. These and subsequent analyses were performed in R 3.3.0.

2.3. Model fitting to simulated data

To better understand the relationships between our five parameters and two response variables, we chose to summarize the response variables as functions of the parameters. The goal of this analysis was not to claim that these functional forms represent underlying mechanisms, but rather to condense the behavior of the response variables into simple yet comprehensive representations. To do this, we investigated how the relationship between the amount of food found by a forager (*F*) and the percent cover of food in a landscape (*PC*) varied with simulated movement parameters, α, *R* and θ, and patch size, μ. In general, the relationship between *F* and *PC* followed a linear-logarithmic functional form (Appendix C). We then used linear regression to explore how changes in simulated movement parameters influenced the shape of the linear-logarithmic fit.

2.3.1. Food found

We demonstrate in Appendix C that for both a forager with no sensory perception in any landscape and a forager with poor sensory perception in a sparse landscape, we would expect *F* to be linear with respect to *PC*. However, for a forager with strong sensory perception in a dense landscape, we would expect *F* to exhibit sublinear behavior with respect to *PC*, because increasing food availability in this scenario will only marginally increase the probability of finding food. Based on these expectations, we chose to compare linear, logarithmic, and piecewise linear-logarithmic functions of *F* with respect to *PC* and found that the piecewise function was best as determined by the coefficient of determination (R^2, see Appendix C). The piecewise 'lin-log' function was defined as:

$$F(PC) = \begin{cases} a(PC) & \text{for } PC \leq c \\ b\log\left(\frac{PC}{c}\right) + ac & \text{for } PC > c \end{cases} \quad (4)$$

where a and b are coefficients to be fit and c is the point of transition between linear behavior and logarithmic behavior. We fit a and b for fixed values of c over the entire range of *PC* values in steps of 0.01%, choosing the value of c that minimized the root mean squared error of the fit (Fig. 2A). Variance on the estimate of c was approximated by bootstrapping ($n = 200$). To explore the relative roles of α, *R*, μ, and θ in determining$a$, b and c, we performed multiple linear regressions with α, *R*, and μ as fixed, continuous factors and θ as a fixed, categorical factor; purely additive models were used.

2.3.2. Benefit-cost ratio

Eq. 4 summarizes the behavior of *F* with respect to *PC*, μ, α, *R*, and. We show in Appendix A that BCR can be approximated as a function of *F* and α, and so the behavior of *BCR* with respect to *PC*, μ, *R*, and θ can be deduced directly from the behavior of *F*.

2.4. Hypothesis generation

Our final aim was to use pre-existing data from a well-studied model organism to generate testable hypotheses about that organism's foraging behavior. To be a good fit to our model, we required an animal with limited memory that forages for sessile food items in a 2-dimensional environment. We chose to use the intertidal common limpet, *Patella vulgata*.

P. vulgata lives on temperate, rocky shores on the west coast of northern Europe and can reach 25 mm in shell length (Hill, 2008). It clings to the rock on which it lives with a large, muscular foot and, much like a terrestrial snail, locomotes by undulating over a layer of

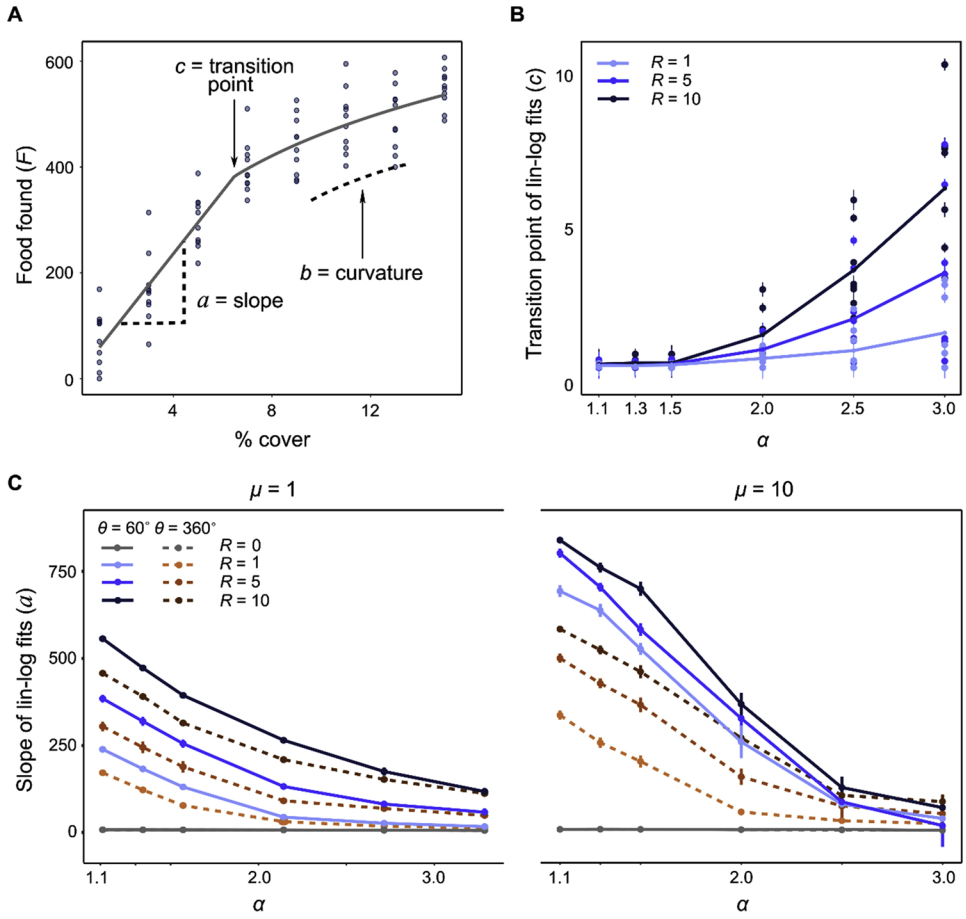

Fig. 2. Fitting functions to observed *F* values. (A) Components *a*, *b*, and *c* of an example lin-log fit to *F* data. (B) The transition point between linear and logarithmic functions, *b*, with respect to α and *R*. (C) The linear slope *a* with respect to α, *R*, μ, and θ.

secreted pedal mucus (Cook, 1969). It forages for both microscopic and macroscopic algae during high tide (Cook, 1969) and travels an average path distance of 0.4 m during foraging (Hartnoll and Wright, 1977). Because of its relatively simple neurological structure (3 major paired ganglia located throughout the body) (Pelseneer, 1906), it is generally assumed that *P. vulgata*'s foraging patterns are not determined by memory. In addition, a recent study examined the step length distributions of 15 individual *P. vulgata* during 9 nocturnal low tides, and fit their step lengths to exponential, power law, and three- and four-tier Weierstrassian Lévy Walk (WLW) models (Reynolds et al., 2017). Of the distributions that we consider here, the authors found that a power law with an exponent near 1 was the best model. This suggests that *P. vulgata* is a good fit to our agent-based model, and provides us with some background information with which to form further hypotheses: For example, *P. vulgata*'s range of sensory perception, and the food distribution in its habitat, remain uncharacterized.

There is sufficient energetic data available in the existing literature to convert the *BCR* values from our simulations into values specific to *P. vulgata*. According to Burrows et al. (Burrows et al., 2000), the standing crop of microalgae available to *P. vulgata* individuals has an energetic content between 0.1 and 0.5 J/mm^2. If we set the scale of our landscapes to 0.5 m x 0.5 m, then each square in the grid is 1 mm x 1 mm, and this energetic content yields 0.1 – 0.5 J per square of food consumed. Additionally, Davies et al. (Davies et al., 1990) calculated that 23% of consumed energy is employed in mucus production, the primary cost of limpet locomotion. They also found the energetic content of mucus to be 8.984 kJ/g. Finally, Davies & Williams (Davies & Williams, 1995) found that a closely-related intertidal limpet, *Cellana grata*, produces between 2.1 and 15.2 µg of mucus per millimeter traveled. If we assume that food was high-quality and travel required little mucus, then our rescaled *BCR* value is:

$$BCR_{P.\ vulgata} = \frac{F(0.5)(0.23)}{D(2.1)(8.984)} \quad (8)$$

If we assume that food was low-quality and travel required little mucus, then our rescaled *BCR* value is:

$$BCR_{P.\ vulgata} = \frac{F(0.1)(0.23)}{D(2.1)(8.984)} \quad (9)$$

After converting *BCR* to values relevant to *P. vulgata*, we examined the foraging parameters (*PC*, μ, α, *R*, and θ) that resulted in energetically viable behavior ($BCR_{P.\ vulgata} \geq 1$). There were no viable *BCR* values for scenarios in which travel required large quantities of mucus (15.2 µg/mm).

3. Results

3.1. Effects of model parameters

In general, food found (*F*) increased with increasing food availability (*PC* and μ). Within this framework, we expected that foraging strategy, α, would have the largest effect on foraging success, followed by radius (*R*) and angle (θ) of sensory perception. Instead, *R* was the largest contributor to variation in *F* (Fig. 3). As expected, larger *R* values resulted in larger quantities of food found (Fig. 4). The power law exponent, α, was the next-largest contributor, with smaller α values generally resulting in more food found. Finally, θ contributed the least amount of variation; increasing θ from 60° to 360° increased the

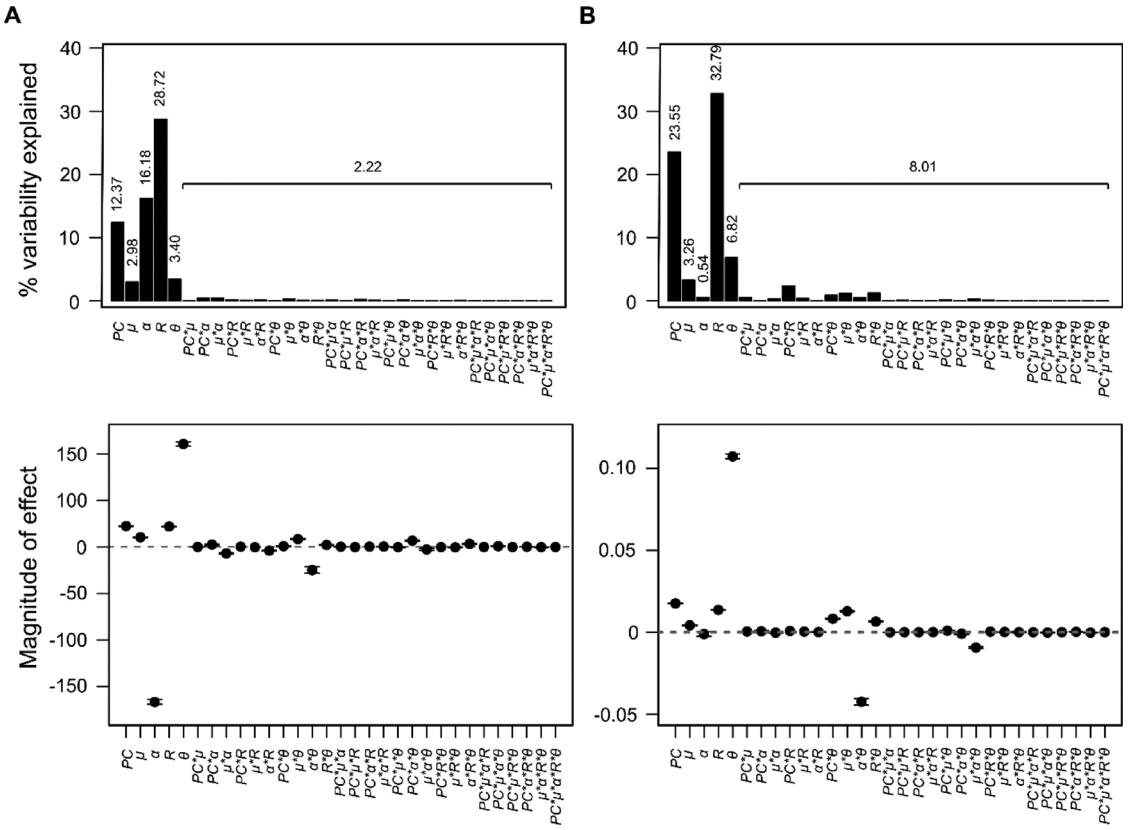

Fig. 3. ANOVA and linear regression results for *F* and *BCR*. The top row shows the percent variation explained by each factor and the interactions between factors for *F* (A) and *BCR* (B). The bottom row shows the regression coefficients for each factor and the interactions between factors for *F* and *BCR*. The coefficients represent change in the response variable per unit change in the relevant factor. Error bars are ± SE.

quantity of food found. The main effects of *PC*, μ, α, *R*, and θ explained 63.66% of the variance in *F*; interaction terms explained only an additional 2.22%.

BCR also increased with increasing percent cover (*PC*) (Fig. 3). As was the case with food found, radius of sensory perception (*R*) contributed most to variation in *BCR*, and *BCR* increased with increasing *R*. Angle of sensory perception, θ, was the second-largest contributor to variation, but increasing θ from 60° to 360° only increased *BCR* when μ or *R* were large and α was small (Fig. 4). Finally, α contributed the least amount of variation to *BCR*. When $R > 0$, smaller α values resulted in larger *BCR*. However, contrary to expectations, larger values of α were best when $R = 0$. The main effects of *PC*, μ, α, *R*, and θ explained 66.95% of the variance in *BCR*; interaction terms explained an additional 8.01%.

We expected that lower values of α would result in larger benefit-cost ratios when *R/NND* was near 0, but that this trend would disappear as *R/NND* approached and exceeded 1. To evaluate this hypothesis, we plotted *BCR* as a linear function of α for each value of μ and θ, and each category of *R/NND* (Fig. 5). We found that $\alpha = 1.1$ did indeed maximize *BCR* when $0.018 < R/NND \leq 0.12$, and that the slope of the relationship between *BCR* and α became more negative as μ and θ increased from 60° to 360°(Table S.2). We also expected that the slope of the relationship between *BCR* and α would approach 0 as *R/NND* approached and exceeded 1. In general, when $\theta = 360°$, the data conformed to this hypothesis. However, slopes did not increase monotonically with *R/NND*. Instead, slopes of intermediate values of *R/NND* ($0.12 < R/NND \leq 0.73$, $0.73 < R/NND \leq 2.42$) tended to be more negative than those at the lowest values. When $\theta = 60°$ and $\mu < 5$, the slopes of the relationships between *BCR* and α were statistically indistinguishable from 0 (Table S.2). When $\mu \geq 5$, slopes were largest when *R/NND* exceeded 1, and were positive (i.e., $\alpha = 3$ outperformed $\alpha = 1.1$).

3.2. Functional form analysis

3.2.1. Food found

Our analysis of food found (*F*) using eq. 4 allowed us to address how *PC*, μ, α, *R*, and θ affected the shape of the relationship between *F* and *PC*. The transition point between linear and logarithmic behavior, *c*, of each fit to our model data increased as α increased and decreased as *R* increased; θ and μ had no significant effect (Fig. 2B). Our linear regression of *c* on *R*, α, μ, and θ yielded coefficients of -0.26 ($p < 0.001$), 2.00 ($p < 0.001$), -0.001 ($p = 0.981$) and -0.04 ($p = 0.919$) respectively. The slope of each lin-log fit, decreased with increasing α, and increased with increasing *R*, μ, and θ (Fig. 2C). Our linear regression of *a* on *R*, α, μ, and θ yielded coefficients of 17.03 ($p < 0.001$), -211.49 ($p < 0.001$), 12.02 ($p < 0.001$) and 92.91 ($p < 0.001$), respectively. Finally, the log coefficient *b* increased with higher values of α; *R*, μ, and θ had no significant effect. Our linear regression of *b* on *R*, α, μ, and θ yielded coefficients of 0.15 ($p = 0.81$), 49.66 ($p < 0.001$), -1.74 ($p = 0.14$), and 2.87 ($p = 0.73$) respectively.

3.2.2. Benefit-cost ratio

As *BCR* can be approximated as a function of *F* and α, in which *BCR* increases monotonically with *F* for a given α value (Appendix A), we did not conduct an additional analysis of *BCR* as a function of *PC*.

3.3. Hypotheses regarding P. vulgata foraging

When we assumed low food quality and low cost of travel, after averaging across replicate simulations, we obtained 27 combinations of *PC*, μ, α, *R*, and θ that resulted in energetically viable foraging ($BCR_{P.\ vulgata} \geq 1$). In this scenario, foragers required $\theta = 360°$, and relatively high *PC* (9% or greater), μ (5 or greater), and *R* (10 or greater) to be viable. However, all α values were indistinguishably effective.

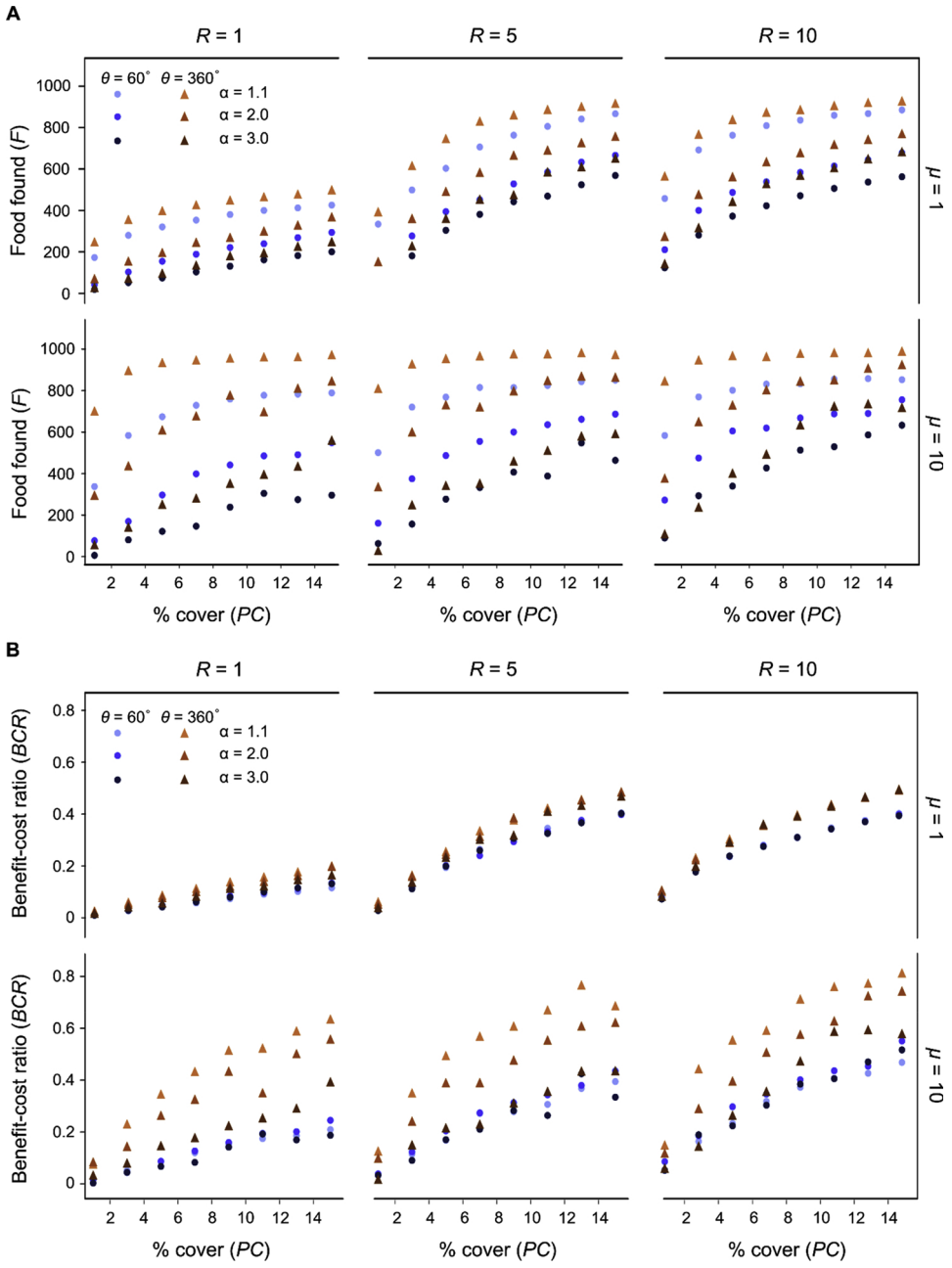

Fig. 4. *F* and *BCR* as functions of *PC* demonstrate the effects of μ, α, *R* and θ, and their interactions, on foraging success. Panel (A) shows *F* plotted against *PC* for $\alpha = 1.1$ (light shade), $\alpha = 2.0$ (medium shade), and $\alpha = 3.0$ (dark shade) for $R = 1$, $R = 5$, and $R = 10$. $\mu = 1$ is shown in the first row; $\mu = 10$ is shown in the second row. Panel (B) shows the same information, but for *BCR* instead of *F*. In both panels, simulations where $\theta = 60^{\circ}$ are in shades of blue; simulations where $\theta = 360^{\circ}$ are in shades of orange.

When we assumed high food quality and low cost of travel, after averaging across replicate simulations, we obtained 1,339 combinations of parameters that resulted in energetic viability. Of these simulations, none included $R = 0$ (Fig. 6). However, for foragers with $R > 0$, viable simulations existed for all *PC* values. Foragers with $\theta = 360^{\circ}$ were able to forage more effectively at lower *PC*, especially if α was also low and the landscape had large food patches. However, for foragers with $\theta = 60^{\circ}$, all α values were indistinguishably effective, especially if *R* was large (greater than 5) and the landscape had smaller food patches.

4. Discussion

Our results suggest that a forager's movement strategy, as defined by the power law exponent α, is the least important contributor to foraging success when the energetic costs of movement are taken into account (*BCR*). Instead, food availability (*PC*) and the forager's range of sensory perception (*R*) are the most important quantities to consider. In addition, the degree to which α affects *BCR* depends on the size of food patches (μ), the forager's angle of sensory perception (θ), and the ratio of the forager's range of sensory perception to the distance between food patches (*R/NND*). In general, α matters most when food patches are large, the forager's angle of sensory perception is unbiased, and *R/NND* is approximately between 0 and 2. Finally, when appropriately parameterized, our model generates testable hypotheses on how animals may optimally interact with their environments while foraging, taking into account food distribution, range of sensory perception, and energetic expenditures.

4.1. Effect of model parameters on foraging success

Our linear regression and analysis of variance results indicate that the

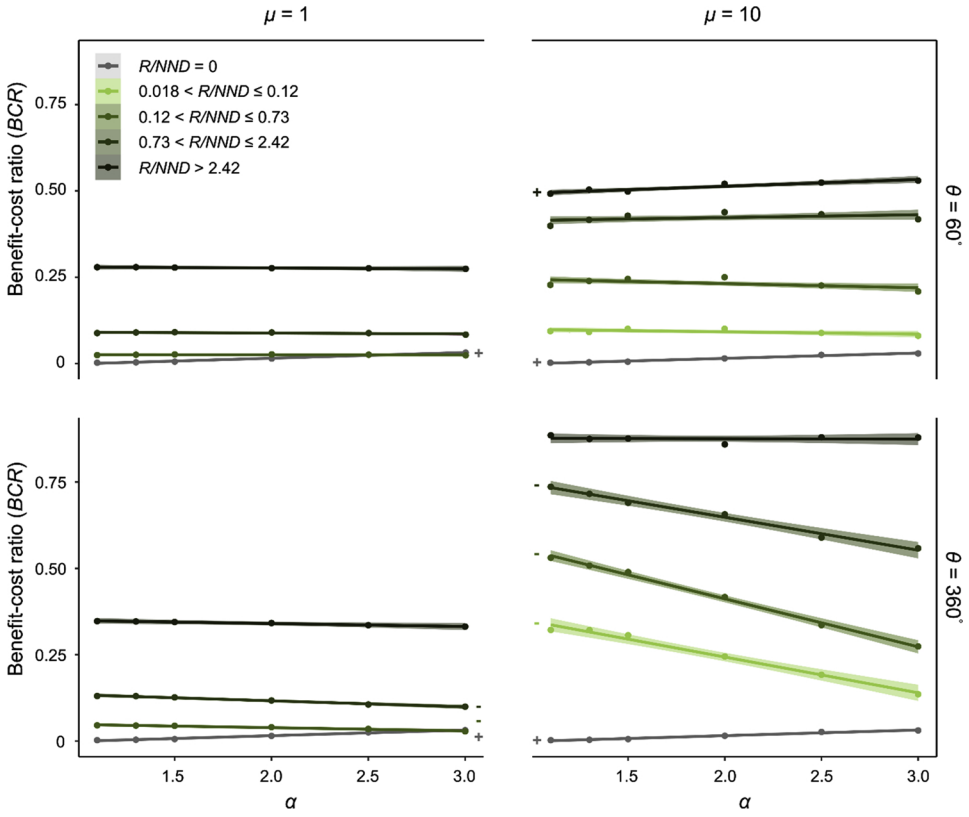

Fig. 5. The effect of α on *BCR* for different *R/NND* values. Benefit-cost ratio is plotted against α for all combinations of θ and *R/NND* for $\mu = 1$ and 10. Simulations where *R/NND* = 0 are shown in grey; darker shades of green correspond to larger *R/NND* values. Points represent *BCR* values averaged across percent cover and simulation replicates ($n = 80$), solid lines represent linear regression results, and shaded areas correspond to ± SE. Lines indicated by + signs have significantly positive slopes; lines indicated by - signs have significantly negative slopes.

power law exponent α should be given reduced emphasis in future studies characterizing the optimal foraging of animals. Quantifying α as a measure of optimality in foraging behavior is a simple and general approach that is understandably compelling, because it is relatively easy to measure from animal track data, which is becoming increasingly available (Wilmers et al., 2015). In addition, other methods to infer underlying behaviors from these data are still very much in development (Dodge et al., 2013; Fleming et al., 2016; Jonsen et al., 2005; Warwick-Evans et al., 2015). Measuring the exponent α provides a simple starting point and a general theoretical framework from which to form further hypotheses. However, we believe it may be misleading to evaluate the optimality of an animal's foraging strategy purely based on its exponent's value. Our data suggest that it would be more informative to characterize an animal's foraging environment and its ability to perceive food sources from a distance, in addition to its movement patterns.

Our model is distinct from Viswanathan et al.'s original simulation (Viswanathan et al., 1999, 2000) in several ways: we incorporated correlated turn angles and variation in food availability, food patch size, and range and angle of sensory perception. A prior study found that broader turn angle distributions and turn angles that were more correlated through time resulted in increased foraging efficiency (Bartumeus et al., 2008a). Based on this, our use of a narrower turn

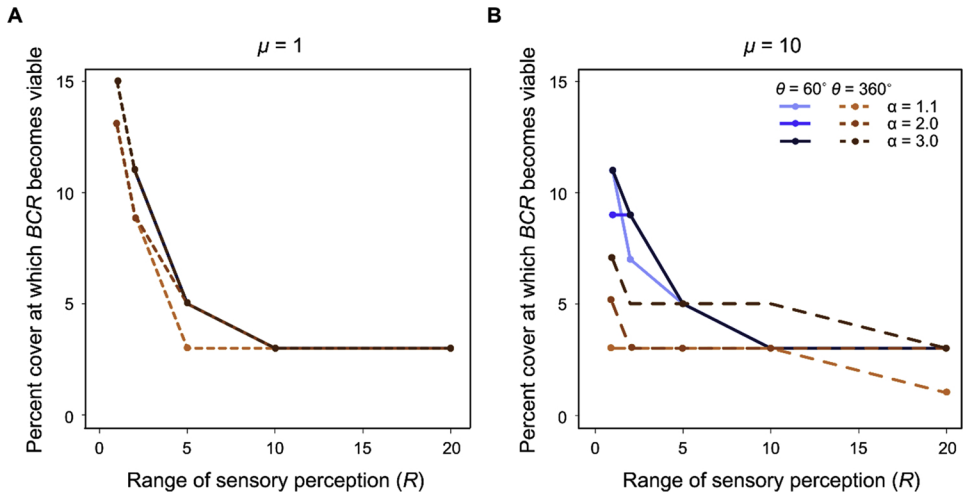

Fig. 6. Minimal viable percent cover values for *P. vulgata*. The lowest *PC* at which $BCR_{P.\,vulgata} \geq 1$ is plotted against *R* for $\alpha = 1.1$ (light shade), $\alpha = 2.0$ (medium shade), and $\alpha = 3.0$ (dark shade). Values from simulations with $\theta = 360^{\circ}$ are in orange, and are connected by dashed lines. In (A), $\mu = 1$; in (B), $\mu = 10$.

angle distribution and turn angles that were correlated across successive time steps should have decreased and increased foraging efficiency respectively. However, since these changes were applied across all of our simulations, the effects of turn angle distribution and correlation should be systematic, and our results that consider the relative effects of PC, μ, α, R, and θ should remain comparable with prior work. With respect to variation in food availability, Bartumeus et al. (2008b) determined that increasing food availability decreased the degree to which an α value near 1 outperformed $\alpha = 3$. They also found that the degree to which α near 1 outperformed $\alpha = 3$ was decreased when food patches were smaller relative to the forager's range of sensory perception. Our results corroborate both of these findings.

Variation in angle of sensory perception has not previously been explored in the literature; it has generally been assumed that all animals perceive food equally well in all directions (e.g. Bartumeus et al., 2008a; Pyke, 2015; Viswanathan et al., 1999, 2000). However, recent work has called for the incorporation of anisotropic and even context-dependent perceptual ranges in foraging models (Olden et al., 2004). We found that narrowing a forager's angle of sensory perception from 360° to 60° resulted in an overall decrease in *BCR*, especially when patch sizes were larger and α values were smaller. It is important to note that we did not test the effects of intermediate values of θ, and therefore cannot fully define the relationship between it and *BCR*. However, this result remains worthy of consideration because many animals do not sense their environments equally well in all directions, but rather have most of their sensory structures located anteriorly (Pelseneer, 1906). Given the impact of a reduced angle of sensory perception on foraging success, it may be an informative addition to future simulations.

It has long been acknowledged that the ratio of radius of sensory perception to the distance foragers must travel between food patches (*R/NND* in our case) is an important indicator of foraging success (e.g. Benhamou, 2007; Raposo et al., 2003; Santos et al., 2004; Viswanathan et al., 1999, 2000, 2011 and others). Essentially, when this ratio is greater than or equal to 1, the forager should be able to perceive its next food patch from its current location. However, prior studies have only reported results from a limited range of ratios (from approximately $1/10^4$ to 1/10) (Bartumeus et al., 2008a, 2008b; Viswanathan et al., 1999, 2000). From this earlier work, researchers concluded that α has the largest effect on foraging success at small ratios, and that this effect becomes negligible as α approaches 1 (Bartumeus et al., 2008a, 2008b; Santos et al., 2004; Viswanathan et al., 1999, 2000). In this study, we chose to explore this relationship explicitly, testing *R/NND* values between approximately 0.02 and 34. Our results generally confirmed prior work; the slope of a linear regression of *BCR* against α becomes less negative and approaches 0 as *R/NND* increases. However, this increase in slope was nonlinear, and in some cases, $\alpha = 3$ outperformed $\alpha = 1.1$. In particular, this occurred when *R/NND* was large, and angle of sensory perception was anteriorly biased. These results suggest that there are intermediate *R/NND* ratios where α values are more or less important to foraging success, and that the assumption that all α values are always equally effective when $R/NND > 1$ is inaccurate.

4.2. Hypothesis generation

Our model was designed to explore the relative contributions of foraging strategy (power law exponent) and range of sensory perception (R, θ) to foraging success in a range of simulated environments, but it can also be used as a hypothesis-generation mechanism for particular organisms and environments. To illustrate this, we used existing data on the energetics of the intertidal limpet, *Patella vulgata*, to parameterize our model. We were able to hypothesize, given a range of food qualities and energetic movement costs, under which food distributions and foraging strategies *P. vulgata* might be energetically viable ($BCR_{P.\ vulgata} \geq 1$). Because the foraging strategies of *P. vulgata* have recently been characterized (Reynolds et al., 2017), we can compare our results with empirical data.

Reynolds et. al (2017) examined the step length distributions of 15 individual *P. vulgata* during 9 nocturnal low tides, and fit them to exponential, power law, and three- and four-tier Weierstrassian Lévy Walk (WLW) models. Of these distributions, the three-tier WLW model was the best fit to the data. WLW models are outside the scope of this study, however, of the models we consider here, Reynolds et al. (2017) determined that a power law with $\alpha \approx 1$ was best. For this α value and a small patch size ($\mu = 1$), our model suggests that *P. vulgata* foraging would be energetically viable at $R = 2$ and $PC = 15\%$, or at $R \geq 10$ and $PC = 3\%$, regardless of angle of sensory perception. Increasing patch size would generally lower the *PC* at which foraging becomes viable, and when patches are large ($\mu = 10$), $\theta = 360°$ would allow for viable foraging at lower *PC*, even when *R* is small.

Note that scenarios in which $\theta = 60°$ are likely better models of *P. vulgata* foraging success. Limpets, like many other animals, possess an anterior concentration of sensory structures, and may not be able to perceive food equally well in all directions. However, our data show that $\theta = 360°$ would generally allow *P. vulgata* to be energetically viable with less food in its environment. It is possible that these observations represent a trade-off between the benefit of finding more food when $\theta = 360°$, and the cost of supporting, for instance, sensory structures that are more equally distributed across the body.

We observed no scenarios in which a high energetic cost of limpet movement (15.2 μg mucus/mm) was energetically viable, however, our results represent the worst-case scenario in terms of the energetics of limpet movement. Many species, including *P. vulgata*, have been observed following mucus trails previously laid down by themselves, by conspecifics, and even by members of other limpet species (Chelazzi et al., 1988; Cook et al., 1969; Cook, 1969; Davies & Hawkins, 1998; Denny, 1989; Funke, 1968; Ng et al., 2013). These mucus trails may substantially reduce the energetics of limpet movement. Davies & Blackwell (Davies & Blackwell, 2007), for example, found that energy expended on mucus decreased by 70% in the littorine snail *Littorina littorea* when they were following a freshly-laid trail. In addition, Connor (Connor, 1986) estimated that mucus trails generated by *Lottia gigantea*, *L. scabra*, and *L. digitalis* persevere in the rocky, wave-swept intertidal environment for at least 7 days. As such, our results should be taken as a worst-case scenario; 15.2 μg mucus/mm may very well be reduced to an energetically viable value when the prevalence of trail-following, the density of limpets, and the persistence of mucus trails are taken into account.

4.3. Functional form analysis

4.3.1. Food found

A lin-log model for food found as a function of percent cover suggested that foragers exhibited two movement modes: one where food found (*F*) was linear with respect to percent cover (*PC*) and *PC* was low, and one where *F* was sublinear (approximately logarithmic) with respect to *PC* and *PC* was high. The first movement mode's linear accumulation of food was likely a signature of correlated random walk behavior (see Appendix C). When *PC* was low (e.g. 1%), and patch size was large (e.g. 10 units per side), the average distance from a patch to its nearest neighbor was about 45 grid units. This distance was farther than the distance from which any of our foragers could perceive food ($R/NND < 1$), meaning that at least one random step was likely to occur between food patches. The smaller the values of R and θ, the more random steps had to be taken between food patches; α controlled the size of these random steps, and therefore also played a significant role. The second movement mode's logarithmic accumulation of food may indicate diminishing returns. In this mode, *PC* was relatively high, and foragers with $R > 0$ were likely to perceive the next food patch from the current one. Because of this, adding more food squares to the landscape had a lower chance of increasing *F* than if the forager were performing a simple random walk. Visualizing tracks from foragers on high and low *PC* landscapes provided some evidence for this two-mode mechanistic explanation of our results (Fig. 7). However, it is possible that *F* may not retain this lin-log behavior at *PC* values greater than those explored in this study.

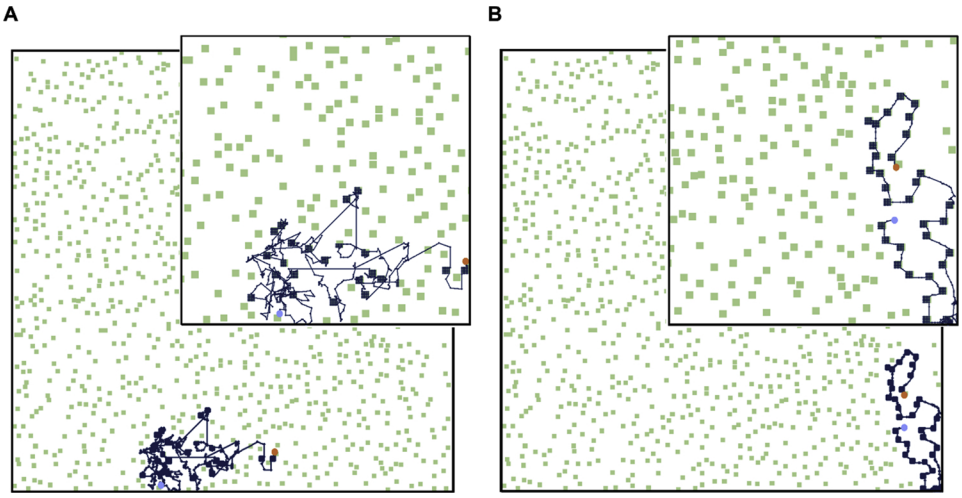

Fig. 7. Example simulated tracks. (A) A track from a forager with $\alpha = 2.0$, $R = 1$, and $\theta = 360^{\circ}$ on a landscape with 11% food cover and $\mu = 5$. This track displays predominantly mode 1 behavior, with many random steps between food patches. (B) A track from a forager with $\alpha = 2.0$, $R = 20$, and $\theta = 360^{\circ}$ on the same landscape as in (A). This track displays predominantly mode 2 behavior, with relatively few, directed steps between food patches.

4.3.2. Benefit-cost ratio

We show in Appendix A that *BCR* can be approximated as a function of F and α, and so the behavior of *BCR* with respect to *PC*, μ, R, and θ can be deduced directly from the behavior of F. Increasing R and μ, or decreasing α, therefore, will increase *BCR* at low *PC*; increasing R or decreasing α will increase the transition point between the two functions; and increasing α will increase *BCR* at high *PC*. However, *BCR* also depends on the average step-length used by the forager ($K(\alpha)$ in equation A.1). This term counteracts the effect of α, increasing *BCR* for smaller average step lengths and decreasing it for larger average step lengths. The opposing effects of α and average step length result in a decreased influence of α on *BCR* relative to its influence on F.

5. Conclusions

Our agent-based model allowed us to explore the relative roles of the power law exponent and sensory perception in efficient foraging, but it did so by making a variety of assumptions about foragers and environmental features that may or may not apply to specific systems. In particular, our model is well-suited for animals that lack spatial memory and forage in environments that can be approximated as 2-dimensional. The assumption of memorylessness is common, especially in invertebrate systems, and many terrestrial and benthic marine and freshwater habitats can be considered 2-dimensional. However, these assumptions and others implicit in our model can be easily altered to suit a variety of research agendas. This is the ultimate power of exploratory agent-based models (ABMs): they are flexible, can be tailored to specific systems, and allow for the cycles of hypothesis generation and testing required to move from observations of animal movement to mechanistic explanations. This repetitive testing is crucial in a field of study where it is increasingly clear that one simple model will not fit all cases (Nathan et al., 2008; Pyke, 2015).

In this study, we conclude that lower values of the power law exponent maximize food found, but that the effect of the exponent on benefit-cost ratio depends strongly on food availability, food patch size, the forager's range of sensory perception, and whether that range is anteriorly-biased. We also suggest that sensory abilities may play a more prominent role in determining foraging success than has previously been acknowledged in the literature. These conclusions lend support to a developing paradigm shift in movement ecology. Researchers are increasingly moving away from simple, probabilistic movement models and exploring agent-based and inferential methods that place more emphasis on how organisms interact with their environments (Benhamou, 2007; Cody, 1971; Nathan et al., 2008; Plank & James, 2008; Pyke, 2015; Reynolds, 2009; Reynolds, 2015; Reynolds, 2018; Siniff & Jesson, 1969). In these models, the "internal state" of the forager is constantly updated with information gleaned from biotic and abiotic features in the environment, and movement patterns – including those that appear to be Lévy or Lévy-like – are emergent properties of this information. As this new paradigm develops, simple models like the one presented here will serve as versatile testing grounds in an iterative, hypothesis-driven experimental process to help determine the key features of organismal movement.

CRediT authorship contribution statement

Diana E. LaScala-Gruenewald: Conceptualization, Methodology, Formal analysis, Data Curation, Writing - original draft, Writing - review & editing, Visualization, Project administration. **Rohan S. Mehta:** Methodology, Validation, Formal analysis, Writing - original draft, Writing - review & editing, Visualization. **Yu Liu:** Methodology, Software, Writing - original draft. **Mark W. Denny:** Resources, Supervision, Writing - review & editing, Funding acquisition.

CRediT authorship contribution statement

Diana E. LaScala-Gruenewald: Conceptualization, Methodology, Formal analysis, Data curation, Writing - original draft, Writing - review & editing, Visualization, Project administration. **Rohan S. Mehta:** Methodology, Validation, Formal analysis, Writing - original draft, Writing - review & editing, Visualization. **Yu Liu:** Methodology, Software, Writing - original draft. **Mark W. Denny:** Resources, Supervision, Writing - review & editing, Funding acquisition.

Acknowledgments

We would like to acknowledge the Santa Fe Institute's Complex Systems Summer School class of 2014 for their participation in the early development of the ideas for this project; G. de Leo, J. Watanabe and P. Roopnarine for their comments on early drafts of our manuscript; and F. King for her help collecting the field data that in part informed our model. Our work was funded by NSF IOS1655529.

Appendix A

A.1 Benefit-cost ratio in terms of food found

Benefit-cost ratio (BCR), as defined by eq. 2, can be written as a function of food found (F). Each of our simulations contained $T = 1000$ time steps, and during each time step, a forager could move between food squares (i.e. "feeding steps"), between food-free squares (i.e. "foraging steps"), or between food and food-free squares. The total distance traveled by the forager is the sum of the distance traveled while feeding and the distance traveled while foraging. If we ignore steps that occur between food and food-free squares, the number of feeding steps will be approximately equal to F, the number of times a food square was encountered. Except for the rare case in which a forager moves between two food patches in a single step, the distance traveled per feeding step is approximately 1, and the distance traveled while feeding is approximately equal to F. The distance traveled while foraging is equal to the average step length drawn from the step length distribution (truncated by the detection of food patches) multiplied by the number of foraging steps ($1000 - F$). The average step length is a function only of α, and does not theoretically exist for the smallest values of α (1.1, 1.3, and 1.5). However, the finite landscape boundary and number of steps drawn from each theoretical distribution result in a defined mean, $K(\alpha)$. Thus, BCR can be written as

$$BCR = \frac{1}{1 + \left(\frac{1000}{F} - 1\right)K(\alpha)} \tag{A1}$$

Both $K(\alpha)$ and F decrease with increasing α. Additionally, eq. 2 indicates that BCR increases with increasing F but decreases with increasing $K(\alpha)$. The effect of α itself on BCR cannot be determined by this method. Because BCR increases with increasing F, the effects of percent cover (PC), patch size (μ), radius of sensory perception (R), and angle of sensory perception (θ) on BCR should be the same as on F.

Appendix B

B.1 Net rate of energy gain in terms of BCR

In OFT, the net rate of energy gain (NREG) is defined as

$$NREG = \frac{energy\ gained}{time} - \frac{energy\ lost}{time} \tag{S6}$$

If we assume our foragers travel at a constant speed s, then our simulation requires one unit of time for each food square found (F) plus the amount of time it takes to travel path length D at speed s. Energy gained in our simulation is proportional to F, and energy lost is proportional to D. Thus, the net rate of energy gain in our simulation is:

$$NREG = \frac{F}{D/s} - \frac{D}{D/s} = s(BCR - 1) \tag{S7}$$

This function monotonically increases with BCR. Note that if one unit of distance travelled costs r units of food found, then the net rate of energy gain is:

$$NREG = \frac{Fs}{Dr} - s = s\left(\frac{BCR}{r} - 1\right) \tag{S8}$$

which still increases monotonically with BCR.

Appendix C

C.1 Rationale for a linear F(PC)

Consider a forager with no sensory perception ($R = 0$) that takes large steps with no directional bias ($\theta = 360^{\circ}$) on a large landscape such that its behavior is approximately nondestructive. The probability that this forager will find food during its next step is approximately independent of whether or not it found food during the previous step. The probability that food is found during the next time step is approximately equal to the food density of the landscape. Thus, the amount of food found by a forager in t foraging steps is the total number of landscape sites visited ($T = 1000$) multiplied by the probability that each landscape site has food ($PC/100$). Thus, in this situation, food found (F) increases linearly with percent cover (PC), with a slope of ˜10.

We plotted F as a function of PC for all simulations in which the forager had no sensory perception ($R = 0$) and observed the predicted linear behavior (Fig A1). We found that our predicted slope of 10 best matched simulations of foragers with smaller values of α. This makes sense, because smaller values of α result in higher probabilities of drawing larger step lengths, which more closely matches our assumptions for linearity and makes it less likely for a forager to revisit a consumed food patch.

C.2 Rationale for a logarithmic F(PC)

For foragers with sensory perception ($R > 0$), we expected to see diminishing returns for increasing values of PC. These foragers do not need to explore large areas of the landscape, and instead tend to fully consume a small area, such that adding more food to the landscape does not improve their foraging efficiency as much as it would a forager lacking sensory perception ($R = 0$). Thus, we would expect to find a sublinear relationship between food found (F) and PC.

We plotted F as a function of PC for all simulations in which the forager had sensory perception ($R > 0$), and observed the predicted logarithmic behavior (see, for example, Fig A1 B).

We found that the logarithmic form best fit the data from foragers with strong sensory perception ($R = 10, 20$). This makes sense, because we

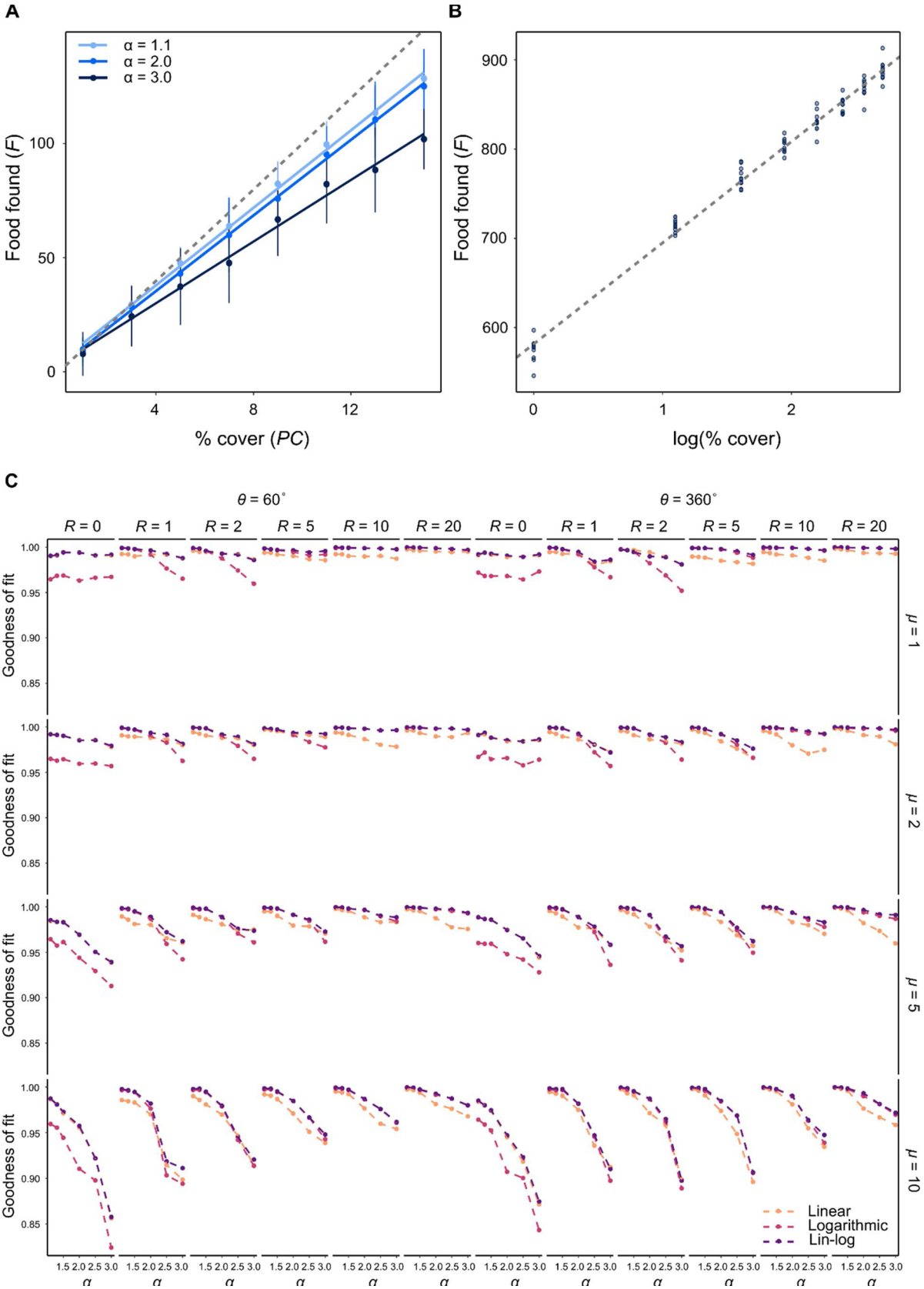

Fig. A1. Linear, logarithmic, and lin-log fits to *F* as a function of *PC*. (A) Linear fit for foragers with no sensory perception ($R = 0$). The dashed line indicates our theoretical prediction of a line with slope 10. (B) Logarithmic fit for a forager with $R = 20$, $\theta = 360^{\circ}$ and $\alpha = 1.3$. (C) Goodness-of-fit (R^2) results for linear, logarithmic, and piecewise linear-logarithmic models for *F(PC)*.

would expect a stronger deviation for a linear pattern to be associated with a stronger deviation from the conditions that should yield that pattern (that is, deviation from $R = 0$).

C.3 Lin-log curve fitting and model selection

Based on the above analytical analyses and our observations of the data, we decided that a linear-logarithmic piecewise function (or 'lin-log') would be a good alternative to purely linear and purely logarithmic models. We fit linear, logarithmic, and lin-log functions to *F(PC)* for each combination of *PC*, α, *R*, μ, and θ we considered. Then, we compared the goodness-of-fit between all three models (Fig A1C). We selected the coefficient of determination, R^2, as our goodness-of-fit measure. We did not penalize for model flexibility (e.g. by using the Akaike Information Criterion) because our goal was purely to summarize our data, and therefore there was no reason to prefer a less flexible model.

See

Appendix D. Supplementary data

Supplementary material related to this article can be found, in the online version, at doi:https://doi.org/10.1016/j.ecolmodel.2019.02.015.

References

Banks, C.J., 1957. The behaviour of individual coccinellid larvae on plants. Br. J. Anim. Behav. 5, 12–24.

Bartumeus, F., Catalan, J., Viswanathan, G.M., Raposo, E.P., da Luz, M.G.E., 2008a. The influence of turning angles on the success of non-oriented animal searches. J. Theor. Biol. 252, 43–55. https://doi.org/10.1016/j.jtbi.2008.01.009.

Bartumeus, F., Fernandez, P., Da Luz, M.G.E., Catalan, J., Solé, R.V., Levin, S.A., 2008b. Superdiffusion and encounter rates in diluted, low dimensional worlds. Eur. Phys. J. Spec. Top. 157, 157–166. https://doi.org/10.1140/epjst/e2008-00638-6.

Bartumeus, F., Giuggioli, L., Louzao, M., Bretagnolle, V., Oro, D., Levin, S., 2010. Fishery discards impact on seabird movement patterns at regional scales. Curr. Biol. 20, 215–222. https://doi.org/10.1016/j.cub.2009.11.073.

Benhamou, S., 2007. How Many Animals Really Do the Lévy Walk? Ecol. Soc. Am. 88, 1962–1969.

Benhamou, S., Bovet, P., 1989. How animals use their environment: a new look at kinesis. Anim. Behav. 38, 375–383. https://doi.org/10.1016/S0003-3472(89)80030-2.

Bond, A.B., 1980. Optimal Foraging in a Uniform Habitat: The Search Mechanism of the Green Lacewing. Anim. Behav. 28, 10–19.

Burrows, M.T., Santini, G., Chelazzi, G., 2000. A state-dependent model of activity patterns in homing limpets: balancing energy returns and mortality risks under constraints on digestion. J. Anim. Ecol. 69, 290–300. https://doi.org/10.1046/j.1365-2656.2000.00391.x.

Chelazzi, G., Focardi, S., Deneubourg, J.-L., 1988. Analysis of Movement Patterns and Orientation Mechanisms in Intertidal Chitons and Gastropods. Behavioral Adaptations to Intertidal Life. Plenum Press New York, pp. 173–184.

Clauset, A., Shalizi, C.R., Newman, M.E.J., 2009. Power-Law Distributions in Empirical Data. SIAM Rev. 51, 661–703. https://doi.org/10.1137/070710111.

Codling, E.A., Plank, M.J., Benhamou, S., 2008. Random walk models in biology. J. R. Soc. Interface 5, 813–834. https://doi.org/10.1098/rsif.2008.0014.

Cody, M.L., 1971. Finch flocks in the Mohave Desert. Theor. Popul. Biol. 2, 142–158. https://doi.org/10.1016/0040-5809(71)90012-8.

Connor, V.M., 1986. The Use of Mucous Trails by Intertidal Limpets to Enhance Food Resources. Biol. Bull. 171, 548–564.

Cook, A., Bamford, O.S., Freeman, J.D.B., Teideman, D.J., 1969. A study of the homing habit of the limpet. Anim. Behav. 17, 330–339. https://doi.org/10.1016/0003-3472(69)90019-0.

Cook, S.B., 1969. Experiments on homing in the limpet Siphonaria normalis. Anim. Behav. 17, 679–682.

Davies, M.S., Blackwell, J., 2007. Energy saving through trail following in a marine snail. Proc. R. Soc. B Biol. Sci. 274, 1233–1236. https://doi.org/10.1098/rspb.2007.0046.

Davies, M.S., Hawkins, S.J., 1998. Mucus from Marine Molluscs, Advances in Marine Biology. Elsevier Masson SAShttps://doi.org/10.1016/S0065-2881(08)60210-2.

Davies, M.S., Hawkins, S.J., Jones, H.D., 1990. Mucus production and physiological energetics in Patella vulgata L. J. Molluscan Stud. 56, 499–503. https://doi.org/10.1093/mollus/56.4.499.

Davies, M.S., Williams, G.A., 1995. Pedal mucus of a tropical limpet, Cellana grata (Gould): energetics, production and fate. J. Exp. Mar. Bio. Ecol. 186, 77–87. https://doi.org/10.1016/0022-0981(94)00156-8.

de Jager, M., Weissing, F.J., Herman, P.M.J., Nolet, B.A., Koppel, J., Van De, 2011. Levy walks evolve through interaction between movement and environmental complexity. Science 80 (332), 1551–1553. https://doi.org/10.1159/000101067.

Denny, M.W., 1989. A limpet shell shape that reduces drag: laboratory demonstration of a hydrodynamic mechanism and an exploration of its effectiveness in nature. Can. J. Zool. 67, 2098–2106. https://doi.org/10.1139/z89-299.

Dodge, S., Bohrer, G., Weinzierl, R., Davidson, S., Kays, R., Douglas, D., Cruz, S., Han, J., Brandes, D., Wikelski, M., 2013. The environmental-data automated track annotation (Env-DATA) system: linking animal tracks with environmental data. Mov. Ecol. 1, 1–14. https://doi.org/10.1186/2051-3933-1-3.

Dray, S., Royer-Carenzi, M., Calenge, C., 2010. The exploratory analysis of autocorrelation in animal-movement studies. Ecol. Res. 25, 673–681. https://doi.org/10.1007/s11284-010-0701-7.

Edwards, A.M., 2008. Using likelihood to test for Lévy flight search patterns and for general power-law distributions in nature. J. Anim. Ecol. 77, 1212–1222. https://doi.org/10.1111/j.1365-2656.2008.01428.x.

Edwards, A.M., Phillips, R. a, Watkins, N.W., Freeman, M.P., Murphy, E.J., Afanasyev, V., Buldyrev, S.V., da Luz, M.G.E., Raposo, E.P., Stanley, H.E., Viswanathan, G.M., 2007. Revisiting Lévy flight search patterns of wandering albatrosses, bumblebees and deer. Nature 449, 1044–1048. https://doi.org/10.1038/nature06199.

Fielden, L.J., Perrin, M.R., Hickman, G.C., 1990. Feeding ecology and foraging behaviour of the Namib Desert golden mole, Eremitalpa granti namibensis (Chrysochloridae). J. Zool. London 220, 367–389. https://doi.org/10.1111/j.1469-7998.1990.tb04313.x.

Fleming, C.H., Fagan, W.F., Mueller, T., Olson, K.A., Leimgruber, P., Calabrese, J.M., 2016. Estimating where and how animals travel: an optimal framework for path reconstruction from autocorrelated tracking data. Ecology 97, 576–582.

Franks, N.R., Richardson, T.O., Keir, S., Inge, S.J., Bartumeus, F., Sendova-Franks, A.B., 2010. Ant search strategies after interrupted tandem runs. J. Exp. Biol. 213, 1697–1708. https://doi.org/10.1242/jeb.031880.

Funke, W., 1968. Heimfindevermogen und 0rtstreue bei Patella L. (Gastropoda, Prosobranchia). Oecologia 2, 19–142.

Hartnoll, R.G., Wright, J.R., 1977. Foraging movements and homing in the limpet Patella vulgata L. Anim. Behav. 25, 806–810. https://doi.org/10.1016/0003-3472(77)90034-3.

Hassell, M.P., May, R.M., 1973. Stability in Insect Host-Parasite Models. J. Anim. Ecol. 42, 693–726.

Hill, J., 2008. Patella vulgata Common limpet. In: Tyler-Waters, H., Hiscock, K. (Eds.), Marine Life Information Network: Biology and Sensitivity Key Information Reviews. Marine Biological Association of the United Kingdom, Plymouth.

Houston, A.I., Mcnamara, J.M., 2014. Foraging currencies, metabolism and behavioural routines. J. Anim. Ecol. 83, 30–40. https://doi.org/10.1111/1365-2656.12096.

James, A., Plank, M.J., Edwards, A.M., 2011. Assessing Levy walks as models of animal foraging. J. R. Soc. Interface 8, 1233–1247.

Jonsen, I.D., Flemmings, J.M., Myers, R. a., 2005. Robust State – Space Modeling of Animal Movement Data. Ecology 86, 2874–2880. https://doi.org/10.1890/04-1852.

Kareiva, P.M., Shigesada, N., 1983. Analyzing Insect Movement as a Correlated Random Walk. Oecologia 56, 234–238. https://doi.org/10.2307/1937543.

Macarthur, R.H., Pianka, E.R., 1966. On Optimal Use of a Patchy Environment. Am. Nat. 100, 603–609.

Mueller, T., Fagan, W.F., Grimm, V., 2011. Integrating individual search and navigation behaviors in mechanistic movement models. Theor. Ecol. 4, 341–355. https://doi.org/10.1007/s12080-010-0081-1.

Nathan, R., Getz, W.M., Revilla, E., Holyoak, M., Kadmon, R., Saltz, D., Smouse, P.E., 2008. A movement ecology paradigm for unifying organismal movement research. Proc. Natl. Acad. Sci. 105, 19052–19059. https://doi.org/10.1073/pnas.0800375105.

Ng, T.P.T., Saltin, S.H., Davies, M.S., Johannesson, K., Stafford, R., Williams, G.A., 2013. Snails and their trails: the multiple functions of trail-following in gastropods. Biol. Rev. 88, 683–700. https://doi.org/10.1111/brv.12023.

Olden, J.D., Schooley, R.L., Monroe, J.B., Poff, N.L., 2004. Context-dependent perceptual ranges and their relevance to animal movements in landscapes. J. Anim. Ecol. 73, 1190–1194.

Pelseneer, P., 1906. A treatise on zoology part v: mollusca. Charles Black, Adam &amp.

Plank, M., James, A., 2008. Optimal foraging: Levy pattern or process? J. R. Soc. Interface 5, 1077–1086. https://doi.org/10.1098/rsif.2008.0006.

Pyke, G.H., 2015. Understanding movements of organisms: It's time to abandon the Lévy foraging hypothesis. Methods Ecol. Evol. 6, 1–16. https://doi.org/10.1111/2041-210X.12298.

Pyke, G.H., 1984. Optimal Foraging Theory: A Critical Review. Annu. Rev. Ecol. Syst. 15, 523–575.

Pyke, G.H., 1978. Optimal foraging: movement patterns of bumblebees between inflorescences. Theor. Popul. Biol. 13, 72–98.

Raichlen, D. a., Wood, B.M., Gordon, A.D., Mabulla, A.Z.P., Marlowe, F.W., Pontzer, H., 2013. Evidence of Levy walk foraging patterns in human hunter-gatherers. Proc. Natl. Acad. Sci. U. S. A. 1–6. https://doi.org/10.1073/pnas.1318616111.

Railsback, S.F., Grimm, V., 2011. Agent-Based and Individual-Based Modeling: A

Practical Introduction. Princeton University Press.
Raposo, E.P., Buldyrev, S.V., da Luz, M.G.E., Santos, M.C., Stanley, H.E., Viswanathan, G.M., 2003. Dynamical robustness of Levy search strategies. Phys. Rev. Lett. 91. https://doi.org/10.1103/PhysRevLett.91.240601.
Reynolds, A.M., 2018. Current status and future directions of Lévy walk research. Biol. Open 7. https://doi.org/10.1242/bio.030106.
Reynolds, A.M., 2015. Liberating Lévy walk research from the shackles of optimal foraging. Phys. Life Rev. 14, 59–83. https://doi.org/10.1016/j.plrev.2015.03.002.
Reynolds, A.M., 2009. Adaptive Lévy walks can outperform composite Brownian walks in non-destructive random searching scenarios. Phys. A Stat. Mech. its Appl. 388, 561–564. https://doi.org/10.1016/j.physa.2008.11.007.
Reynolds, A.M., Santini, G., Chelazzi, G., Focardi, S., 2017. The Weierstrassian movement patterns of snails. R. Soc. Open Sci. 4.
Reynolds, A.M., Schultheiss, P., Cheng, K., 2014. Does the Australian desert ant Melophorus bagoti approximate a Lévy search by an intrinsic bi-modal walk? J. Theor. Biol. 340, 17–22. https://doi.org/10.1016/j.jtbi.2013.09.006.
Root, R.B., Kareiva, P.M., 1984. The search for resources by cabbage butterflies (Pieris rapae): ecological consequences and adaptive significance of Markovian movements in a patchy environment. Ecology 65, 147–165. https://doi.org/10.2307/1939467.
Santos, M.C., Raposo, E.P., Viswanathan, G.M., Da Luz, M.G.E., 2004. Optimal random searches of revisitable targets: Crossover from superdiffusive to ballistic random walks. Europhys. Lett. 67, 734–740. https://doi.org/10.1209/epl/i2004-10114-9.
Seuront, L., Stanley, H.E., 2014. Anomalous diffusion and multifractality enhance mating encounters in the ocean. Proc. Natl. Acad. Sci. U. S. A. 111, 1–6. https://doi.org/10.1073/pnas.1322363111.
Sims, D.W., Southall, E.J., Humphries, N.E., Hays, G.C., Bradshaw, C.J. a, Pitchford, J.W., James, A., Ahmed, M.Z., Brierley, A.S., Hindell, M. a, Morritt, D., Musyl, M.K., Righton, D., Shepard, E.L.C., Wearmouth, V.J., Wilson, R.P., Witt, M.J., Metcalfe, J.D., 2008. Scaling laws of marine predator search behaviour. Nature 451, 1098–1102. https://doi.org/10.1038/nature06518.
Siniff, D.B., Jesson, C.R., 1969. A simulation model of animal movement patterns. Advances in Ecological Research. Academic Press New York, pp. 185–219.
Smith, J.N.M., 1973. The food searching behaviour of two European thrushes. II: The adaptiveness of the search patterns. Behaviour 49, 1–60.
Tang, W., Bennett, D., 2010. Agent based Modeling of Animal Movement: A Review. Geogr. Compass 4, 682–700. https://doi.org/10.1111/j.1749-8198.2010.00337.x.
Thomas, G., 1974. The influences of encountering a food object on subsequent searching behaviour in Gasterosteus aculeatus L. Anim. Behav. 22, 941–952. https://doi.org/10.1016/0003-3472(74)90017-7.
Turchin, P., 1998. Quantitative analysis of movement: measuring and modeling population redistribution in animals and plants Vol. 1 Sinauer Associates Sunderland.
Viswanathan, G.M., Afanasyev, V., Buldyrev, S.V., Havlin, S., da Luz, M.G.E., Raposo, E.P., Stanley, H.E., 2000. Levy flights in random searches. Physica A 282, 1–12.
Viswanathan, G.M., Buldyrev, S.V., Havlin, S., da Luz, M.G.E., Raposo, E.P., Stanley, H.E., 1999. Optimizing the success of random searches. Nature 401, 911–914. https://doi.org/10.1038/44831.
Viswanathan, G.M., Da Luz, M.G.E., Raposo, E.P., Stanley, H.E., 2011. The physics of foraging: an introduction to random searches and biological encounters. Cambridge University Press.
Warwick-Evans, V., Atkinson, P., Gauvain, R., Robinson, L., Arnould, J.P.Y., Green, J., 2015. Time-in-area represents foraging activity in a wide-ranging pelagic forager. Mar. Ecol. Prog. Ser. 527, 233–246. https://doi.org/10.3354/meps11262.
Weimerskirch, H., Bonadonna, F., Bailleul, F., Mabille, G., Dell'Omo, G., Lipp, H.-P., 2002. GPS tracking of foraging albatrosses. Science 80 (295), 1259. https://doi.org/10.1126/science.1068034.
White, J., Tobin, T., Bell, W.J., 1984. Local search in the housefly Musca domestica after feeding on sucrose. J. Insect Physiol. 30, 477–487.
Wilmers, C.C., Nickel, B., Bryce, C.M., Smith, J.A., Wheat, R.E., Yovovich, V., 2015. The golden age of bio-logging: how animal-borne sensors are advancing the frontiers of ecology. Ecology 96, 1741–1753.
With, K.A., King, A.W., 1999. Dispersal success on fractal landscapes. Landsc. Ecol. 14, 73–82.
Zollner, P.A., Lima, S.L., 1999. Illumination and the perception of remote habitat patches by white-footed mice. Anim. Behav. 58, 489–500.